METROLOGY AT THE HEART OF TODAY'S TECHNOLOGIES

Station de Mesure on-Wafer Nano-Robotisée Assistée par IA : Automatisation, Précision et Évaluation des Performances

AI-Enhanced Nano-Robotic Wafer Measurement Station: Automation, Precision, and Performance Evaluation

Clément Lenoir[1], Mohamed Sebbache[1], Daouda Seck[1,2], Djamel Allal[2], Kamel Haddadi[1]

[1]Univ. Lille, CNRS, Centrale Lille, Univ. Polytechnique Hauts-de-France, UMR 8520 - IEMN - Institut d'Électronique de Microélectronique et de Nanotechnologie, IRCICA USR-3380, F-59000 Lille, France {kamel.haddadi@univ-lille.fr}
[2]Laboratoire National de Métrologie et d'Essais, Paris, France.

Mots clés: Mesures sous pointes hyperfréquences, Calibration, Nano-robotique, Intelligence artificielle
Index Terms: Microwave on-wafer measurements, Calibration, Nano-robotics, Artificial intelligence

Résumé/Abstract

This work presents a nano-robotic on-wafer probe station integrating an AI-assisted vision system to optimize probe alignment and enhance measurement precision. Machine vision algorithms optimize probe positioning, reduce measurement errors, and enhance reproducibility. Real-time image data processing and pattern matching enable adaptive calibration for robust performance under varying conditions. Preliminary results show significant improvements in speed and accuracy over conventional methods. This approach offers a next-generation solution for precise on-wafer RF measurement.

Ce travail présente une station de mesure sous-pointes nano-robotisée intégrant un système de vision assistée par IA, permettant des mesures entièrement automatisées et de haute précision. Des algorithmes de vision par ordinateur optimisent le positionnement des sondes, réduisent les erreurs de mesure et améliorent la répétabilité. Le traitement en temps réel des images et la reconnaissance de motifs permettent une calibration adaptative pour une performance robuste dans des conditions variables. Les résultats préliminaires montrent des améliorations significatives en termes de rapidité et de précision par rapport aux méthodes conventionnelles. Cette approche constitue une solution de nouvelle génération pour la mesure RF de précision sous-pointes.

1 Introduction

High-frequency characterization of micro- and nano-electronic devices relies on on-wafer RF probe stations. Traditionally, these stations are manually operated or semi-automated, making measurements prone to alignment errors, operator-dependent accuracy, and difficult-to-control variability. These limitations become critical as device complexity increases, operating frequencies rise, and industrial demands grow for precision, repeatability, and automation.

Over the last two decades, the semiconductor industry has witnessed a continuous trend toward device miniaturization, in accordance with Moore's Law and beyond. Today's integrated circuits routinely incorporate components with sub-10 nm features and operate at millimeter-wave and even terahertz frequencies. This scaling down has pushed the performance envelope but also magnified the sensitivity of RF measurements to even the slightest misalignment or probing error. As a result, traditional probe stations—designed for larger, less sensitive structures—struggle to meet the precision and repeatability required at these scales. Simultaneously, the demand for high-throughput and highly reproducible characterization has grown with the advent of 5G, 6G, advanced radar systems, quantum computing, and heterogeneous integration platforms. These technologies impose strict constraints on RF measurement uncertainty, especially in scenarios where impedance mismatches or parasitic effects can significantly distort results. Manual or semi-automated stations are increasingly becoming bottlenecks in terms of speed, accuracy, and operational consistency.

Manual probe positioning leads to variability in alignment, increased measurement errors, and limited reproducibility [1], [2]. The process is time-consuming, requiring skilled technicians to ensure proper calibration and probing accuracy. Furthermore, such setups lack adaptability for the delicate probing of advanced high-

frequency devices, where fine RF quantities need to be reliably extracted [3], [4]. These shortcomings highlight the urgent need for a fully automated, high-precision solution.

In this context, the integration of advanced technologies such as nano-robotics, computer vision systems, and artificial intelligence offers a promising alternative. These technologies not only automate repetitive and delicate tasks but also significantly improve alignment precision and result reliability. Through real-time image recognition and pattern analysis, probe positioning can be dynamically optimized, reducing human errors and operator-induced variability.

To address these challenges, we present a fully automated on-wafer probe station that integrates nano-positioners and an AI-assisted machine vision system. The system enables automatic calibration based on advanced image recognition algorithms and precise detection of probe-to-substrate contact. This paper describes the mechanical and software architecture of the station, the operation of the vision system, the positioning algorithms, and preliminary experimental results using an ISS 101-190-C impedance standard.

2 Architecture of the Measurement Station

2.1 Overview of the Architecture

The proposed measurement station is a fully automated platform designed for high-precision RF probing, with a particular focus on Ground-Signal-Ground (GSG) alignment. This system is built from scratch. The station integrates various components, each serving a distinct function but all contributing to the seamless operation of the measurement process. These components include two independently controlled probe arms, a nano-robotized wafer chuck, piezoelectric nanorobotic positioners, and an advanced optical and mechanical setup [5][6] [7] [8].

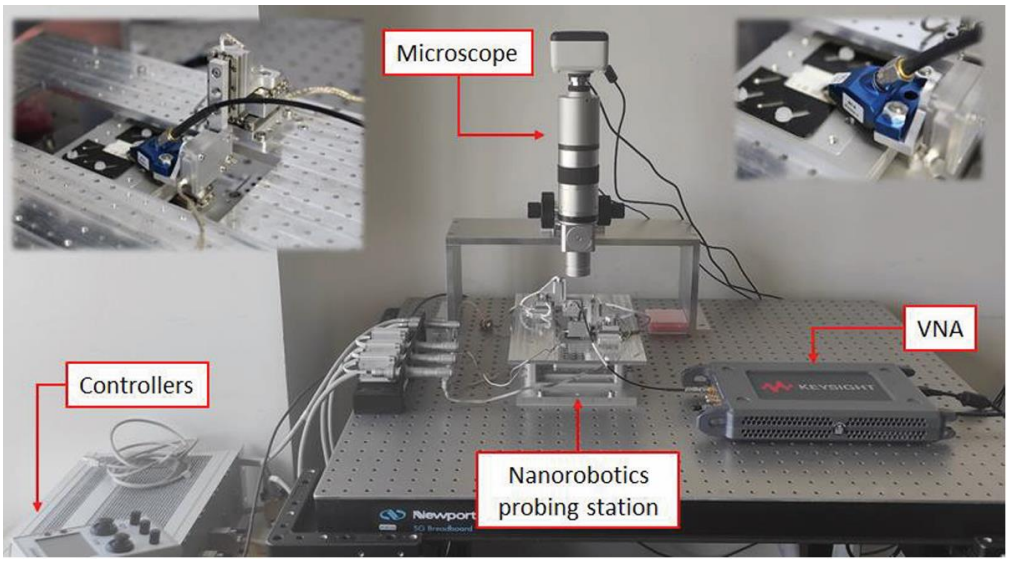

Figure 1. Nano-robotic on-wafer RF probe station.

The mechanical base of the station is a Newport® M-VIS3036-SG2-325A optical table, with volume 750 × 900 × 59 mm³, equipped with pneumatic isolators that offer horizontal and vertical isolation at 5 Hz and 10 Hz, respectively, ensuring 90% and 98% vibration isolation. This feature is crucial in mitigating building vibrations and enhancing the overall stability of the measurement process.

At the heart of the measurement process, a Keysight® 5008A Streamline Series USB Vector Network Analyzer (VNA) is used to measure S-parameters across a frequency range from 100 kHz to 53 GHz. The compact design of the Streamline VNA facilitates its integration directly onto the optical table, minimizing cable lengths and reducing associated measurement uncertainties. The system leverages LabVIEW® for full automation, providing seamless control over the measurement process. Flexible MegaPhase® UltraPhase cables, with a 30 cm length and an operating frequency of up to 67 GHz, are used to connect the VNA to the probes. These cables are chosen for their light weight, flexibility, and minimal signal attenuation, ensuring that no excessive tension is applied to the positioners.

To assist with precise probe-to-pad alignment, a Moticam® CAM-1080P HDMI camera, with 2 MP resolution and 60 frames per second at 1080p, is mounted above the probing area. This camera, coupled with a Moticam dedicated software, enables real-time image acquisition and facilitates calibration for dimensional measurements. Additionally, a Moticam OP-Z10 Zoom Microscope, offering optical magnification from 0.85x to 8.5x, provides detailed visual feedback for probe positioning, with a resolution down to 2.5 µm. A SmarAct® MCS2 controller coordinates the positioning system, with closed-loop control providing high precision. The system includes a total of 11 stages for controlling the probe arms and chuck, enabling fine-tuned adjustments in both translation and rotation. Furthermore, custom attachment pieces, designed using SolidWorks®, ensure secure mounting of FormFactor® Infinity GSG probes onto the positioners, addressing the mechanical challenges posed by the probes' geometry.

2.2 Nano-robotic Actuation System

The measurement station employs SmarAct® piezoelectric nano-positioners, specifically selected for their resolution, repeatability, and compact design. These nano-positioners, crucial for high-precision RF probing, are employed in the control of both the probe arms and the chuck. Each probe holder is mounted on a stack of SmarAct stages, enabling precise control along the X, Y, Z, and θ axes. Meanwhile, the chuck is positioned using three stages—two linear and one rotational—providing three degrees of freedom (DoF) in X, Y, and φ axes. The probes themselves are mounted on four stages—three linear and one rotational—allowing four degrees of freedom (DoF) in X, Y, Z, and θ axes.

The SmarAct stages used in the system are part of the SLC and SR series, specifically designed for closed-loop operation with integrated capacitive sensors, ensuring sub-nanometer resolution. The linear stages, such as the SLC-17 and SLC-24 models, provide exceptional rigidity and straightness, with travel ranges of 16–21 mm and resolution down to 1 nm. For rotational motion, the SR series stages provide continuous, unrestricted rotation, with resolutions of 25 µ° for the probe stages and 15 µ° for the chuck.

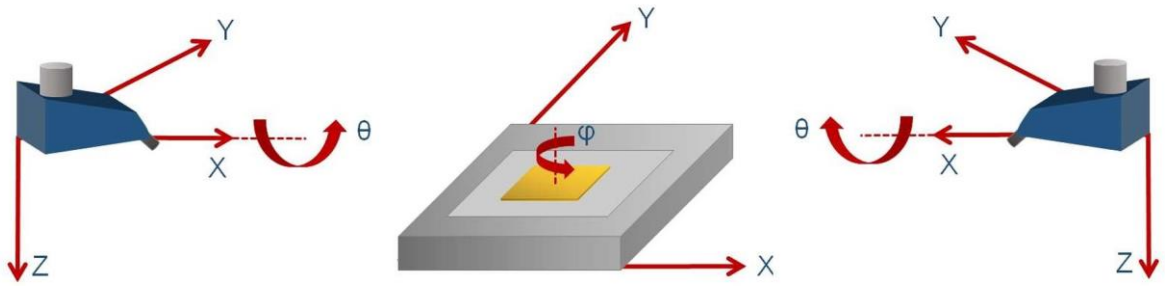

Figure 2. Visualization of the 11 nano-positionners DOFs.

This setup ensures that the system achieves high precision in positioning, essential for repeatable and accurate RF measurements. With closed-loop control, the nano-positioners can maintain stable positioning over extended periods, even when subject to external factors such as cable tension or mechanical vibrations.

2.3 Description of the ISS 101-190-C Standard

The ISS 101-190-C calibration substrate, developed by FormFactor®, is widely recognized in the RF metrology community for its precision and reliability. It is designed to facilitate Short-Open-Load-Thru (SOLT) calibrations in coplanar waveguide (CPW) configurations, offering well-defined reference structures, clearly marked alignment targets, and consistent geometries that are essential for automated vision-based detection and alignment.

In our station, the automation for alignment and calibration is currently limited to the use of the ISS 101-190-C substrate. This approach was chosen for simplicity and reproducibility, enabling smooth integration with the existing positioning and control systems. The ISS 101-190-C provides a standardized and well-documented interface, making it easier to automate the calibration process.

2.4 Software Control and Automation

LabVIEW™ serves as the central hub for the automation process, managing the entire sequence of operations from image recognition to positioner movements and VNA control. The automated system operates as follows:

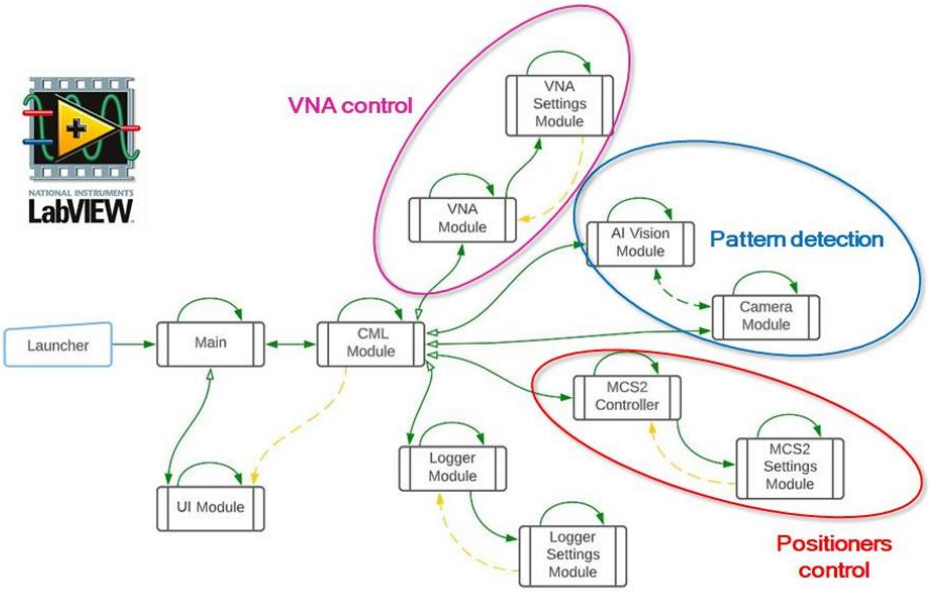

Figure 3. LabVIEW algorithm modules tree.

Image Recognition and Positioning: The first step in the process is pattern detection, which is achieved using a combination of the camera module and the AI Vision module. The camera module links the camera to LabVIEW™, managing the camera's settings and parameters. The AI Vision module is a dedicated LabVIEW component that handles image recognition, including template matching and alignment. These modules work together to detect the position of the ISS 101-190-C calibration substrate and the corresponding pads for the probes.

Positioner Control: Once the correct position has been identified through image recognition, the system uses the MCS2 Settings module to configure the SmarAct® positioners. This module defines the settings for each of the stages (probe and chuck positioners), and the MCS2 controller executes the movement commands, adjusting the positioners in X, Y, Z, and θ/φ directions. The positioners are precisely controlled to ensure alignment with the DUT (Device Under Test) as per the predefined parameters.

VNA Integration and Data Acquisition: The VNA control module includes the VNA Settings module, which manages the configuration of the Keysight® 5008A Streamline Series VNA. This module sends commands to trigger measurements and acquire data once the positioners are correctly aligned. The VNA module in LabVIEW™ executes these commands and saves the measurement results for further analysis.

3 Computer Vision and Artificial Intelligence for Probe Alignment

3.1 Pattern Recognition Algorithms

The vision system relies exclusively on NI Vision Assistant for pattern matching to identify the positions of the probes and calibration elements on the ISS 101-190-C calibration substrate. The process begins with the capture of high-resolution images of the calibration substrate and the probes, followed by real-time image processing using template-based pattern matching techniques.

In this context, template matching is used to locate key features, such as the tips of the probes and the various calibration standards (open, short, load, and thru) on the substrate. The system compares predefined templates of these features against the captured images. By calculating the similarity between the template and regions within the image, it accurately identifies the positions of the probes and calibration structures.

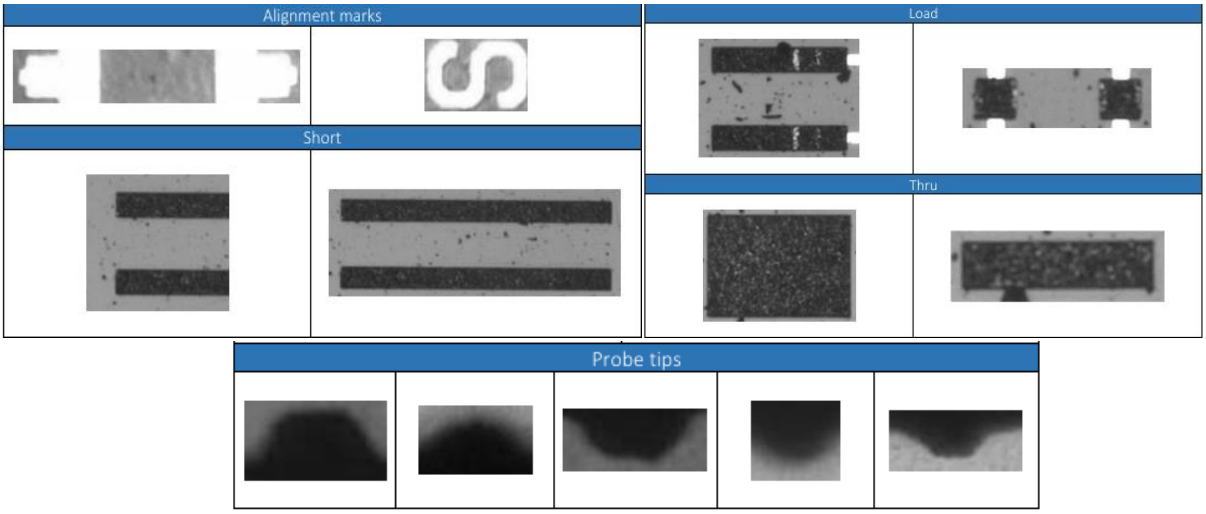

Figure 4. Sample pictures used as template for the machine vision module.

NI Vision Assistant provides an intuitive environment for configuring these pattern matching routines. The templates for each probe and calibration element are created manually, ensuring that the system can recognize these features in different image frames. The matching algorithm then identifies the best match based on pattern similarity, giving precise locations of the probe tips and calibration structures. Once the positions of these features are determined, the system can calculate alignment corrections in the X, Y, and θ axes. These corrections are then transmitted to the SmarAct® controllers, which adjust the positioning of the probes accordingly, ensuring precise alignment with the calibration standards.

3.2 Positioning Logic

The positioning of the probes and chuck is guided by a set of precise calculations and algorithms that utilize the results from the machine vision system. The key objective is to achieve accurate alignment of the probes with the calibration structures on the ISS 101-190-C substrate, ensuring repeatable and reliable measurements.

To achieve this, the system divides each calibration standard and probe structure into three key sections. This segmentation allows for the creation of reference lines, which are essential for determining the relative alignment of the probes. For the calibration standards, the system identifies a central line that runs through the standard, and similarly, for the probes, it identifies the three distinct points (or "teeth") of the probe tips. These three points are used to construct a reference line for each probe.

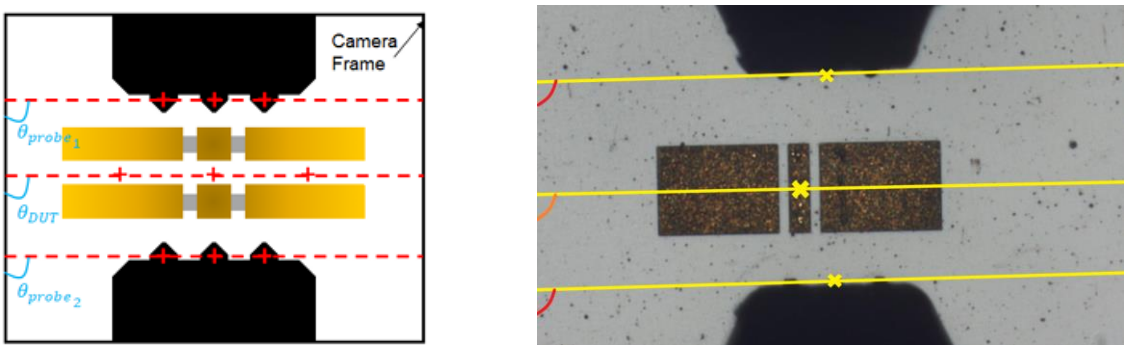

Figure 4. Automatic probe positioning and angular corrections.

Once the reference lines for both the standards and probes are established, the system calculates the angular difference between the probe lines (both upper and lower probes) and the corresponding lines of the standards. This angular deviation serves as the basis for further adjustments. The positioning algorithm then calculates the necessary adjustments required to bring the probes into precise alignment with the standards. This process involves a combination of P control loops and other fine-tuning algorithms to ensure smooth and accurate movements of

the positioning stages. The P controller helps to minimize the error between the current position of the probes and the target positions by adjusting the speed and acceleration of the stages in real-time. Additionally, a set of safety protocols is implemented to prevent any potential damage to the equipment. These safety mechanisms monitor the motion of the stages and ensure that they do not exceed defined limits, avoiding issues such as collisions or overtravel. If any irregularities are detected, the system halts movement immediately, ensuring the safety of both the DUT and the probing equipment.

This combination of precise calculation, real-time control, and safety measures ensures that the system operates with both high precision and reliability, minimizing errors and preventing mechanical issues during the alignment process.

3.3 Contact Detection via Image Feedback

Beyond static alignment, the vision system also plays a crucial role in detecting physical contact between the probe tips and the DUT. Contact is primarily identified by monitoring changes in the optical signature of the probe tip, such as deformation or change in reflectivity, and by analyzing motion discontinuities in the Z-axis. Overtravel refers to the continued downward movement of the probe tip after initial contact with the DUT, while skating describes the lateral movement of the probe tip on the wafer surface as a result of overtravel. In our system, these phenomena are differentiated by analyzing the movement patterns of the probe. If a downward motion in the Z-axis (indicating probe approach) is accompanied by a simultaneous movement of the probe in the X-axis, this indicates lateral motion (skating) of the probe tip along the surface.

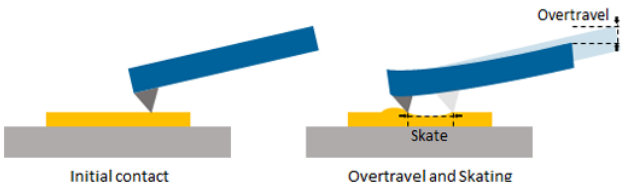

Figure 5. Overtravel and skating principle

This image-based contact detection is supplemented with real-time feedback from the SmarAct positioning stages, which allows precise monitoring of probe movement in all axes. By correlating Z-axis motion with X-axis visual displacement, the system can accurately identify when skating occurs, thus confirming probe contact. The combination of optical feedback and positional data provides a robust, real-time approach to avoid overtravel and minimize the risks of probe damage or inaccurate measurements. This technique has proven highly repeatable in identifying probe contact moments, ensuring precise and reliable RF probing through multiple contact cycles, even in the presence of skating and overtravel.

3.4 Calibration Routine and Contact Procedure

The procedure for executing a 2-port calibration on the 101-190 C Impedance Standard Substrate (ISS) in relation to the positioner behavior follows a systematic sequence:

Phase 1: In this phase, the system leverages the feedback from the camera and the AI Vision Module to identify the alignment marks on the ISS. Specifically, the center of each alignment mark is located, and the angle between the structure and the camera frame is determined. In addition, the tips of the two probes are detected, with the system calculating their centers and the angle between the line connecting the probe tips and the camera frame's parallel.

Phase 2: Once the alignment marks and probe tips are identified, the probes are aligned based on the coordinates gathered in Phase 1. Using the positioners for the probes and the chuck, the system ensures that the probes' tips are perfectly centered over the structure, with the angle between the probes and the structure set to zero. Following alignment, the probes are lowered until they make good contact with the ISS. The positions of the probes along the X and Y axes are then saved and locked to prevent any further movement.

Phase 3: At this stage, the operator selects one of the four calibration standards. The AI Vision Module will recognize the chosen standard, locating its center and angle in a manner similar to the process in Phase 1.

Phase 4: The standard is then centered in relation to the probes using only the chuck positioners. After the alignment is completed, the probes are lowered, and the measurement is initiated (once the probes touch the surface, an additional overtravel is applied to ensure the probe tips are perfectly aligned with the alignment structure. As recommended by the ISS manufacturer, this overtravel is set to 20 µm. The system automatically detects the initial contact when the probes start to "skate" on the surface, with this value being pre-set manually and incorporated into the program). Following the measurement, the probes are raised, and the chuck is reset. Phases 3 and 4 are repeated for each of the calibration standards.

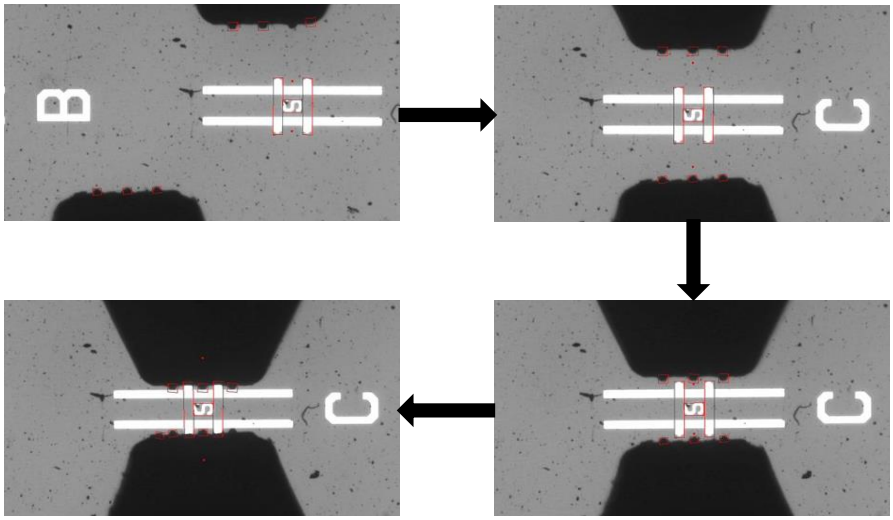

Figure 6. Execution of phase 1 & 2 on an alignment pad.

4 Experimental Results and Performance Evaluation

4.1 Automated SOL Calibration and probe-positioning Protocol

To validate our nano-robotic positioning system, all calibrations were driven by the same control program. We performed ten consecutive SOL calibrations on each of the three standards (open, short, load), under three distinct conditions:

Automated with probe retraction/repositioning, after each calibration cycle the probes were fully retracted and then automatically repositioned on the same target point. Automated in-contact, the probes remained in continuous contact with the standard between cycles (no movement). Manual, **t**he same operator performed ten approach-retract calibration cycles by hand, using a conventional manual probe station.

All ten repetitions for each method were carried out under identical environmental and VNA settings.

4.2 Statistical analysis of calibration residuals

From each calibration trial, we extracted the three VNA error-term residuals, directivity (δ), reflection-tracking (τ), and source-match (µ) and computed their 3σ standard deviations over the 1–50 GHz frequency range. The table below presents a summary of these residual values specifically at 10 GHz for comparison across the three measurement methods.

Residual error	10 GHz		
	3 σ		
	Manual	*In contact Automated*	*In movement Automated*
δ_1	7.4267×10^{-4}	1.1703×10^{-4}	1.4900×10^{-4}
τ_1	2.3201×10^{-3}	4.4022×10^{-4}	5.2248×10^{-4}
μ_1	4.0472×10^{-3}	3.1665×10^{-4}	2.6407×10^{-4}

Figure 7. Residual calibration errors (3σ) at 10 GHz for manual, in-contact & in-movement automated probing methods

Comparable reductions, by roughly one to two orders of magnitude, were seen for τ and μ. Overall, fully automated probe handling (both in-contact and retract-reposition modes) cuts calibration residuals by up to 90% versus manual probing, yielding up to a 40% decrease in total measurement uncertainty.

4.3 Automation Benefits and Performance Metrics

The transition from manual to fully automated probe handling delivers clear operational and safety advantages. By orchestrating every approach–retract and standard-exchange step through a unified control program, the system eliminates most of the subtle misalignments and contact-force fluctuations that inevitably arise when an operator manually adjusts the probes. Automation therefore not only boosts consistency between successive calibrations, but also greatly reduces the risk of occasional probe crashes or substrate scratching. Software safety interlocks continuously monitor tip loading and travel limits; any deviation beyond predefined thresholds triggers an immediate motion halt, preserving both delicate probe tips and valuable wafer samples. Moreover, once a calibration sequence is initiated, the station can proceed through multiple SOL routines without human intervention—freeing human resources from repetitive tasks and allowing them to focus on higher-level analysis rather than manual alignment. These combined improvements in reliability, reproducibility, and hardware protection make the AI-augmented probe station particularly well suited for environments where operator access is limited or where sample throughput and equipment longevity are critical.

5 Conclusion

We have demonstrated an AI-powered, nano-robotic on-wafer probe station that consistently outperforms manual methods in terms of calibration repeatability and hardware safety. Our experiments show dramatic reductions in VNA error-term residuals—directivity, reflection tracking, and source match—when the entire SOL procedure is driven by automated scripts. Safety features and collision-avoidance routines virtually eliminate probe damage and substrate mishandling, while the hands-off operation streamlines workflow and minimizes user-dependent variability. Future work will deepen this validation by extending the range of calibration standards (e.g., thru, line) and measurement frequencies, refining the AI algorithms to adaptively compensate for probe wear, and compiling a larger statistical dataset across multiple device types. These results demonstrate the system's ability to meet the stringent demands of both research laboratories and high-volume RF test facilities.

Acknowledgement

This work was supported, in part by the EPM project 23IND10 OnMicro, in part by the French Renatech network, and in part by the CPER Hauts de France project IMITECH.

References

[1] F. Mubarak *et al.*, "An Interlaboratory Comparison of On-Wafer S-Parameter Measurements up to 1.1 THz," in *IEEE Transactions on Terahertz Science and Technology.*

[2] H. Happy *et al.*, "Measurement Techniques for RF Nanoelectronic Devices: New Equipment to Overcome the Problems of Impedance and Scale Mismatch," in *IEEE Microwave Magazine*, vol. 15, no. 1, pp. 30-39, Feb. 2014.

[3] K. Daffe *et al.*, "On-Wafer Broadband Microwave Measurement of High Impedance Devices-CPW Test Structures with Integrated Metallic Nano-Resistances," *2018 48th European Microwave Conference (EuMC)*, Madrid, Spain, 2018, pp. 25-28.

[4] M. Horibe, "Improvement of Measurement Uncertainty of THz Waveguide Vector Network Analyzers," *2021 96th ARFTG Microwave Measurement Conference (ARFTG)*, San Diego, CA, USA, 2021, pp. 1-4.

[5] C. Mokhtari *et al.*, "Impact of GSG Probe to Pads Contact Repeatability for On-Wafer RF Measurements," *2021 IEEE 7th International Conference on Smart Instrumentation, Measurement and Applications (ICSIMA)*, Bandung, Indonesia, 2021, pp. 241-246

[6] C. Mokhtari *et al.*, "New Generation of On-Wafer Microwave Probe Station for Precision GSG Probing," *2022 24th International Microwave and Radar Conference (MIKON)*, Gdansk, Poland, 2022, pp. 1-4.

[7] C. Mokhtari, *et al.*, "Automated and Robotic On-Wafer Probing Station," *2023 IEEE Symposium on Wireless Technology & Applications (ISWTA)*, Kuala Lumpur, Malaysia, 2023, pp. 99-102

[8] C. Mokthari *et al.*, "Exploring Nanorobotics Integration with Microwave and Millimeter-Wave Techniques for Advanced On-wafer Measurement," *2024 5th International Conference in Electronic Engineering, Information Technology & Education (EEITE)*, Chania, Greece, 2024, pp. 1-6.